Experimental Investigation of High-Energy Photon Splitting in Atomic Fields

Sh. Zh. Akhmadaliev, G. Ya. Kezerashvili, S. G. Klimenko, R. N. Lee, V. M. Malyshev, A. L. Maslennikov, A. M. Milov, A. I. Milstein, N. Yu. Muchnoi, A. I. Naumenkov, V. S. Panin, S. V. Peleganchuk, G. E. Pospelov, I. Ya. Protopopov, L. V. Romanov, A. G. Shamov, D. N. Shatilov, E. A. Simonov, V. M. Strakhovenko, and Yu. A. Tikhonov

Budker Institute of Nuclear Physics, Novosibirsk, 630090, Russia

(Received 18 February 2002; published 19 July 2002)

Data analysis of an experiment in which photon splitting in atomic fields was observed is presented. The experiment was performed at the tagged photon beam of the ROKK-1M facility at the VEPP-4M collider. In the energy region of 120–450 MeV, statistics of 1.6×10^9 photons incident on the BGO target was collected. About 400 candidate photon-splitting events were reconstructed. Within the attained experimental accuracy, the experimental results are consistent with the calculated exact atomic-field cross section. The predictions obtained in the Born approximation differ significantly from the experimental results.

DOI: 10.1103/PhysRevLett.89.061802 PACS numbers: 12.20.Fv, 13.60.Fz, 25.20.Dc

Introduction.—Photon splitting (PS) is a process in which the initial photon turns into a virtual electron-positron pair that scatters in the electric field of an atom and then transforms into two photons sharing the initial photon energy ω_1 (see Fig. 1). This is an example of a self-action of an electromagnetic field, which results also in such effects as coherent photon scattering (Delbrück scattering) and photon-photon scattering. The latter phenomenon was never observed experimentally.

Delbrück scattering (DS) was investigated in detail both theoretically and experimentally [1–3]. It turned out that, for heavy atoms and high photon energy, its cross section calculated exactly in the parameter $Z\alpha$ ($Z|e|$ is the nucleus charge, $\alpha = e^2/4\pi = 1/137$ is the fine-structure constant) drastically differs from that obtained in the lowest order in this parameter (Born approximation).

Recently, essential progress in the understanding of PS phenomena was achieved. In papers [4–6] various differential cross sections of high-energy PS have been calculated exactly in the parameter $Z\alpha$. Similar to the case of Delbrück scattering, the exact cross section turns out to be noticeably smaller than that obtained in the Born approximation. So, the detailed experimental investigation of PS provides a new possibility to verify our understanding of QED in the presence of strong external fields when the effect of higher-order terms is very important.

The observation of PS is a difficult problem due to the smallness of the cross section as compared to those of other processes initiated by the initial photons in a target. The following background processes are significant: double Compton effect off the atomic electrons ($\gamma e \to \gamma\gamma e$), and the emission of two hard photons from the e^+e^- pair produced by the initial photon. The relative importance of these processes depends on the photon energy. For the energy $\omega_1 \sim m$, where the search of PS was undertaken in two experiments [7,8], only double Compton scattering determines the background conditions. In these experiments, the photons from an intense radioactive source (Zn^{65} with $\omega_1 \simeq 1.1$ MeV in [7], and Co^{60} with $\omega_1 \simeq 1.17$, 1.33 MeV in [8]) were used. The combination of the coincidence and energy-summing detection technique was applied. The number of events considered as candidates for PS exceeded the theoretical expectations by a factor of 300 in [8], and by a factor of 6 in [7].

At high photon energy $\omega \gg m$ the emission of hard photons from the e^+e^- pair becomes most important as a background process. In 1973 the experiment devoted to the study of the Delbrück scattering of photons in energy region 1–7 GeV was performed [9]. The bremsstrahlung nontagged photon beam was used. Some events were assigned by the authors of [9] to the PS process. As shown in [10,11], the theoretical value for the number of PS events under the conditions of the experiment was 2 orders of magnitude smaller than the experimental result. It was also argued that the events observed could be explained by the production of the e^+e^- pair and one hard photon.

The first successful observation of photon splitting was performed in 1995–1996 using the tagged photon beam of the energy 120–450 MeV at the VEPP-4M e^+e^- collider at the Budker Institute of Nuclear Physics (Novosibirsk).

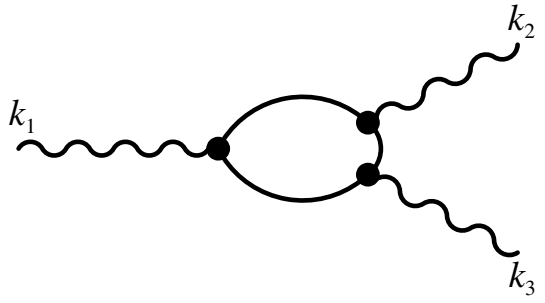

FIG. 1. Feynman diagram for photon splitting. Solid lines correspond to electron propagators in the atomic electric field.

Another goal of this experiment was a study of Delbrück scattering [3]. The total statistics collected was 1.6×10^9 incoming photons with a BGO (bismuth germanate) target and 4×10^8 without a target for background measurements. The preliminary results were published in [12,13]. Here we present the new data analysis for this experiment.

Scheme of experiment.—The experimental setup is shown in Fig. 2. Some ideas for this setup were suggested in [14]. The main features of the experimental approach are as follows.

(i) The use of a high-quality tagged photon beam produced by backward Compton scattering of laser light off a high-energy electron beam. Thereby, the energy of the initial photon is accurately determined.

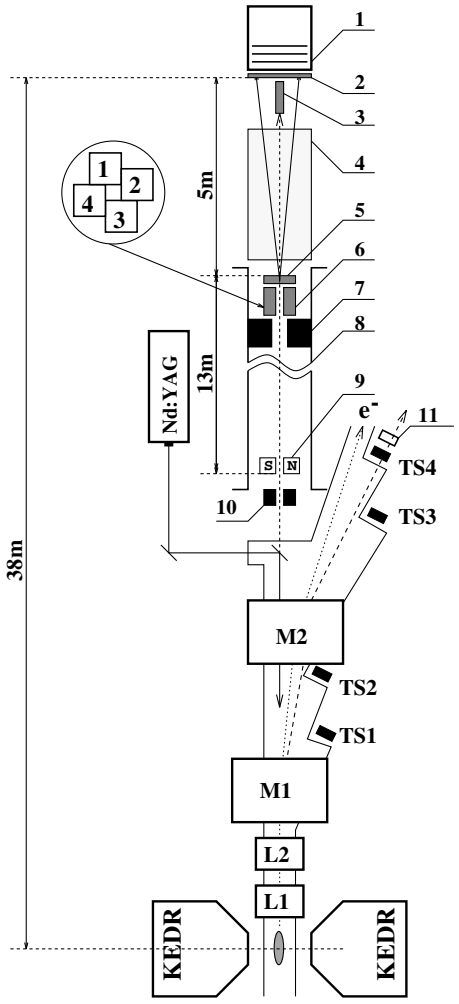

FIG. 2. Principal scheme of setup: LKr calorimeter (1); scintillation veto-counter (2); beam dump (BGO) (3); He-filled tube (4 m length) (4); target (BGO) (5); active collimator (BGO) (6); lead absorber (7); guiding tube for the gamma-quanta beam (8); cleaning magnet (9); passive lead collimator (10); TS scintillation counter (11); Nd:YAG is the laser; TS1–TS4 are tagging system hodoscopes; M1 and M2 are bending magnets; L1 and L2 are quadrupole lenses.

(ii) Strong suppression of the background processes by means of the detection of charged particles produced in the target and in other elements of the photon-beam line.

(iii) The detection of both final photons to discriminate the PS events from those with one final photon produced in Compton or Delbrück scattering.

(iv) The requirement of the balance between the sum of the energies of the final photons and the energy of the tagged initial photon. This provides the additional suppression of the events with charged particles missed by the detection system.

At the high energy of the initial photon $\omega_1 \gg m$, the PS cross section is peaked at small angles between momenta of all photons ($\sim m/\omega_1$). Therefore, a good collimation of the primary photon beam is required. The ROKK-1M facility [15] is used as the intense source of the tagged γ quanta. The electron energy loss in the process of Compton scattering of laser light is measured by the tagging system (TS) [16] of the KEDR detector [17]. The TS consists of the focusing spectrometer formed by accelerator quadrupole lenses and bending magnets, and four hodoscopes of the drift tubes. High-energy photons move in a narrow cone around the electron beam direction. The angular spread is of the order $1/\gamma$, where $\gamma = E_{\text{beam}}/m$ is the relativistic factor of the electron beam. The photon energy spectrum has a sharp edge at

$$\omega_{th} = \frac{4\gamma^2 \omega_{\text{laser}}}{1 + 4\gamma\omega_{\text{laser}}/m} \tag{1}$$

that allows one to perform the absolute calibration of the tagging system in a wide energy range. In experiment the laser photon energy was $\omega_{\text{laser}} = 1.165$ eV, the electron beam energy $E_{\text{beam}} = 5.25$ GeV, and $\omega_{th} = 450$ MeV. The photon energy resolution provided by the tagging system depends on the photon energy and on the position of the scattered electron in the TS hodoscope: it was 0.8% at $\omega_1 = 450$ MeV (at the center of the hodoscope) and $\sim$5% at $\omega_1 = 120$ MeV (at the edge of the hodoscope). The collimation of the photon beam is provided by two collimators spaced at 13.5 m. The last collimator, intended to strip off the beam halo produced on the first one, is made of four BGO (bismuth germanate) crystals as shown in a separate view of Fig. 2. After passing through the collimation system, the photon beam hits $1X_0$ thick BGO crystal target, where X_0 is the radiation length.

All photons outgoing from the target within the cone $\theta \leq \theta_0$ around the initial beam axis are absorbed by the dump made of 13 X_0 thick BGO crystals installed in front of the photon detector. The incoming photons which passed the target without interaction are also absorbed by the dump. For a too large value of θ_0, many photon splitting events would be lost, while for a too small value of θ_0, the noninteracted photons would overwhelm the data acquisition system. Moreover, this dump allows us to suppress the background from the double Compton scattering

of laser photons off the electron beam. As an optimum, the value $\theta_0 = 2.4$ mrad was chosen.

All active elements used in beam line (collimators, target, dump, scintillating veto counter) set a veto signal in the trigger, and their signals are used in the analysis of background suppression. The information from the target and beam dump is also used for measurement of the incoming photon flux. The liquid-krypton ionization calorimeter is used for the detection of the final photons. Its three-layer double-sided electrode structure enables one to get both (X and Y) coordinates for photons having the polar angles in the region $2.4 \leq \theta \leq 20$ mrad. The energy resolution of the calorimeter is $2\%/\sqrt{\omega(\mathrm{GeV})}$. The liquid-krypton calorimeter is described in detail in [18,19].

Results.—In the event selection procedure the following constraints were applied: (i) The absence of the signal caused by charge particles in all active elements of the photon-beam line. (ii) The balance of the tagged initial photon energy and the energy measured in the calorimeter within 3σ of its energy resolution. (iii) The existence of two separate tracks at least for one (X or Y) coordinate in the calorimeter strip structure.

The fulfillment of the latter requirement strongly suppresses the contribution of the processes with one photon in the final state which could imitate two photon events in the calorimeter.

A typical event which meets selection criteria is shown in Fig. 3. In this example two tracks are seen in both X and Y directions. The conversion of the first photon occurs in layer 1, while the second photon converts in layer 2.

The experimental results are presented in Table I and in Figs. 4 and 5 together with the results of Monte Carlo (MC) simulation. In Table I the results of MC simulation using the exact (in $Z\alpha$) as well as Born PS cross sections are shown, along with those for DS and other background processes. The PS cross section used accounts for atomic constituents of the BGO molecule as well as for the effect of screening by the atomic electrons. The energy spectrum

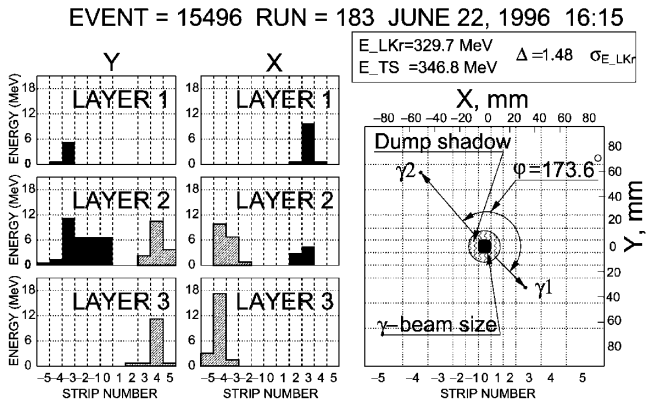

FIG. 3. Energy profile in the calorimeter strip structure (left) and reconstructed kinematics (right) for a typical candidate to the photon splitting event.

TABLE I. The number of reconstructed events. Here Q is the number of incoming photons. $N_{\phi<150^\circ}$ ($N_{\phi>150^\circ}$) is the number of events with the complanarity angle $\phi < 150^\circ$ ($\phi > 150^\circ$) [see Fig. 5(a)], normalized to the experimental statistics collected with the target.

Data	Target	Q, 10^9	$N_{\phi>150^\circ}$	$N_{\phi<150^\circ}$
Experiment	$Bi_4Ge_3O_{12}$	1.63	336 ± 18	82 ± 9
Experiment	no target	0.37	10 ± 3	10 ± 3
MC PS (exact)	$Bi_4Ge_3O_{12}$	6.52	364 ± 10	72 ± 5
MC PS (Born)	$Bi_4Ge_3O_{12}$	6.52	416 ± 10	104 ± 5
MC DS	$Bi_4Ge_3O_{12}$	1.63	3 ± 1.7	17 ± 4
MC other backgr.	$Bi_4Ge_3O_{12}$	1.63	3 ± 1.7	12 ± 3.5

of the initial photons measured in the tagging system is shown in Fig. 4(a). Table I and Fig. 5 present the data summed up over the initial photon spectrum. The errors shown in Table I are statistical ones. The systematic error is determined by the accuracy of the measurement of the number of initial tagged photons and by the uncertainty in the reconstruction efficiency of photon splitting events. The estimation of these systematic errors gives 2% and 5%, respectively.

As seen from Table I and Fig. 5(a), the main part of the PS events has, in agreement with the theory, a complanarity angle φ (the azimuth angle between final photon momenta) close to 180°. The choice of the interval $\varphi > 150^\circ$ allows us to improve the signal-to-background ratio (see, e.g., the last two rows of Table I). Just this φ interval was used to plot the distributions over polar angles in Fig. 5 and the dependence of the number of reconstructed PS events on the initial photon energy E_{TS} in Fig. 4(b). Note that for most of the events in this φ interval, the variable $\tilde{x} = \theta_{\min}/(\theta_{\min} + \theta_{\max})$ is approximately equal to

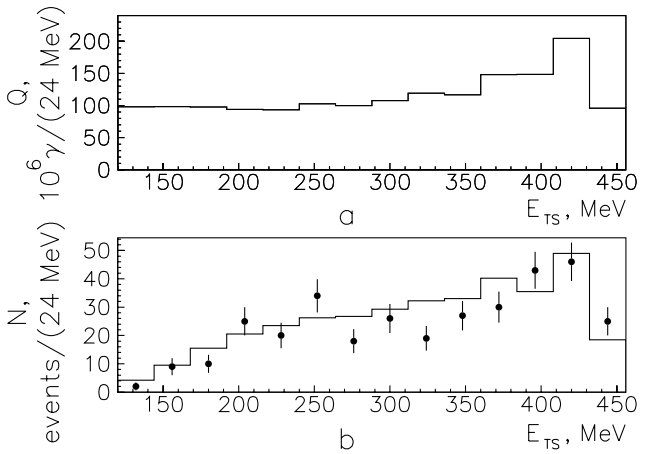

FIG. 4. (a) The photon energy spectrum measured in the tagging system (TS). (b) The number of reconstructed PS events as a function of the tagged photon energy E_{TS}. In plot (b) solid circles present the experimental results, and the histogram is the result of MC simulation using exact formulas.

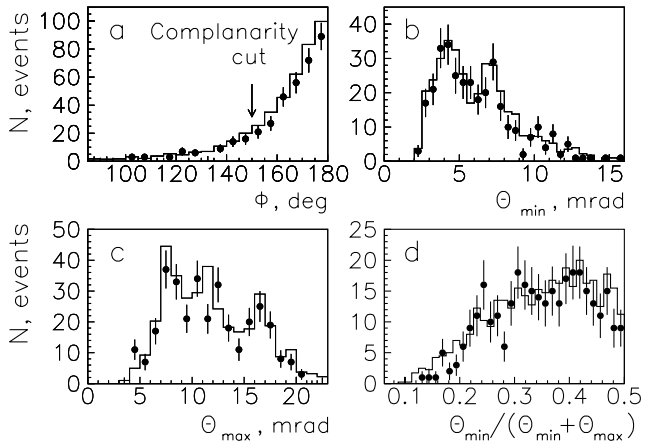

FIG. 5. The number of the selected PS events as a function of the azimuth angle between momenta of the outgoing photons (a), the polar angle $\theta_{\min} = \min\{\theta_2, \theta_3\}$ (b), the polar angle $\theta_{\max} = \max\{\theta_2, \theta_3\}$ (c), and the variable $\tilde{x} = \theta_{\min}/(\theta_{\min} + \theta_{\max})$ (d). In (b), (c), and (d) only events satisfying the complanarity cut $\varphi \geq 150°$ [see (a)] are included. Solid circles present the experimental results, and the histograms are the results of MC simulation using exact formulas.

the ratio $\min(\omega_2, \omega_3)/\omega_1$ since the main contribution to the cross section comes from the region $|\mathbf{k}_{2\perp} + \mathbf{k}_{3\perp}| \ll k_{2\perp}, k_{3\perp}$, i.e., $\varphi \approx 180°$ and $\omega_2\theta_2 \approx \omega_3\theta_3$.

The results presented in Table I and in Figs. 4(b) and 5 show good agreement between the theory and the experiment. More precisely, the total number of reconstructed events in the experiment (see Table I) differs from the result of MC simulation by 1.6 standard deviations.

In order to understand the role of the Coulomb corrections under the experimental conditions, we have compared the visible cross sections calculated exactly in $Z\alpha$ and in the Born approximation. For all photon energies considered, the Born result exceeds the exact one by 20% approximately. As seen from Table I, the use of the Born cross section for MC simulation leads to the disagreement of 3.5 standard deviations between the theory and the experiment. In other words, the experimental results are significantly closer to predictions of the exact theory than to those obtained in the Born approximation.

The results obtained confirm the existence of photon splitting phenomenon. They also make possible the quantitative comparison with the theoretical predictions. Moreover, the attained experimental accuracy allows one to distinguish between the theoretical predictions obtained with or without accounting for the Coulomb corrections. It turns out that the Coulomb corrections essentially improve the agreement between the theory and the experiment. We conclude that the experiment and the theory are consistent within the achieved experimental accuracy.

We are grateful to the staff of the VEPP-4M accelerator complex for reliable work during the data taking. We thank A. N. Skrinsky and V. A. Sidorov for support of this experiment. Partial support by the RFBR (Grant No. 01-02-16926) is also gratefully acknowledged.

[1] P. Papatzacos and K. Mork, Phys. Rep. **21**, 81 (1975).
[2] A. I. Milstein and M. Schumacher, Phys. Rep. **243**, 183 (1994).
[3] Sh. Zh. Akhmadaliev *et al.*, Phys. Rev. C **58**, 2844 (1998).
[4] R. N. Lee, A. I. Milstein, and V. M. Strakhovenko, Zh. Eksp. Teor. Fiz. **112**, 1921 (1997) [Sov. Phys. JETP **85**, 1049 (1997)].
[5] R. N. Lee, A. I. Milstein, and V. M. Strakhovenko, Phys. Rev. A **57**, 2325 (1998).
[6] R. N. Lee, A. I. Milstein, and V. M. Strakhovenko, Phys. Rev. A **58**, 1757 (1998).
[7] A. W. Adler and S. G. Cohen, Phys. Rev. **146**, 1001 (1966).
[8] W. K. Roberts and D. C. Liu, Bull. Am. Phys. Soc. **11**, 368 (1966).
[9] G. Jarlskog *et al.*, Phys. Rev. D **8**, 3813 (1973).
[10] V. N. Baier, V. M. Katkov, E. A. Kuraev, and V. S. Fadin, Phys. Lett. B **49**, 385 (1974).
[11] R. M. Dzhilkibaev *et al.*, JETP Lett. **19**, 47 (1974).
[12] Sh. Zh. Akhmadaliev *et al.*, in *PHOTON'97, Incorporating the XIth International Workshop on Gamma-Gamma Collisions, Egmond-aan-Zee, The Netherlands, 1997* (World Scientific, Singapore, 1998), p. 246.
[13] A.L. Maslennikov, in *Proceedings of the Workshop on Photon Interactions and the Photon Structure, Lund, 1998* (Fysiska Institutionen, Lund, 1999), pp. 347–365.
[14] A. I. Milstein and B. B. Wojtsekhovski, Report No. BINP 91-14, Novosibirsk, 1991.
[15] G. Ya. Kezerashvili *et al.*, Nucl. Instrum. Methods Phys. Res., Sect. B **145**, 40 (1998).
[16] V. M. Aulchenko *et al.*, Nucl. Instrum. Methods Phys. Res., Sect. A **355**, 261 (1995).
[17] V. V. Anashin *et al.*, in *Proceedings of the International Symposium on Position Detectors in High-Energy Physics, Dubna, 1988* (Joint Institute for Nuclear Research, Dubna, 1988), p. 58.
[18] V. M. Aulchenko *et al.*, Nucl. Instrum. Methods Phys. Res., Sect. A **394**, 35 (1997).
[19] V. M. Aulchenko *et al.*, Nucl. Instrum. Methods Phys. Res., Sect. A **419**, 602–608 (1998).